

Research Article

Mid-anaphase arrest in *S. cerevisiae* cells eliminated for the function of Cin8 and dynein

A. Gerson-Gurwitz^a, N. Movshovich^a, R. Avunie^b, V. Fridman^b, K. Moyal^b, B. Katz^a, M. A. Hoyt^c and L. Gheber^{a,b,d,*}

^a Department of Chemistry, Ben-Gurion University of the Negev, Beer-Sheva, 84105 (Israel)

^b Department of Clinical Biochemistry, Ben-Gurion University of the Negev, Beer-Sheva, 84105 (Israel)

^c Department of Biology, Johns Hopkins University, Baltimore, 21218 (USA)

^d Departments of Clinical Biochemistry and Chemistry, Zlotowski Center for Neuroscience, Ben-Gurion University of the Negev, Beer-Sheva, 84105 (Israel), Fax: +972-8-6281361, e-mail: lgheber@bgu.ac.il

Received 10 August 2008; received after revision 22 October 2008; accepted 27 October 2008

Online First 16 December 2008

Abstract. *S. cerevisiae* anaphase spindle elongation is accomplished by the overlapping function of dynein and the kinesin-5 motor proteins, Cin8 and Kip1. Cin8 and dynein are synthetically lethal, yet the arrest phenotypes of cells eliminated for their function had not been identified. We found that at a non-permissive temperature, *dyn1Δ* cells that carry a temperature-sensitive *cin8-3* mutation arrest at mid-anaphase with a unique phenotype, which we named TAN (two microtubule asters in one nucleus). These cells enter anaphase, but fail to proceed through the slow phase

of anaphase B. At a permissive temperature, *dyn1Δ*, *cin8-3* or *dyn1Δcin8-3* cells exhibit perturbed spindle midzone morphologies, with *dyn1Δcin8-3* anaphase spindles also being profoundly bent and non-rigid. Sorbitol, which has been suggested to stabilize microtubules, corrects these defects and suppresses the TAN phenotype. We conclude that dynein and Cin8 cooperate in anaphase midzone organization and influence microtubule dynamics, thus enabling progression through the slow phase of anaphase B.

Keywords. Cin8, dynein, anaphase B, microtubules, sorbitol.

Introduction

Mitotic chromosome segregation is the mechanism by which duplicated genomic information is transmitted to daughter cells during cell division. This essential process is mediated by the mitotic spindle, a highly dynamic microtubule (MT)-based structure which undergoes a distinct set of morphological changes in each mitotic cycle. During anaphase B, the final stage of the bipolar spindle morphogenesis, the spindle

elongates dramatically, thus spatially separating sister chromatids. In *S. cerevisiae* cells, anaphase spindle elongation proceeds in two phases: in the first, a fast phase, the spindle elongates from 1–2 μm to 4–5 μm, and in the second, a slow phase, the spindle elongates up to 7–10 μm [1, 2]. The mechanisms that control the transition between the fast and slow phases have not yet been elucidated. However, it has been shown that proper organization of the spindle midzone, the region of overlap between antiparallel interpolar MTs, becomes critical at this stage as the elimination of the midzone-organizing protein Ase1 prevents progression through the slow phase of anaphase B [3].

* Corresponding author.

In *S. cerevisiae* cells, progression through anaphase spindle elongation requires the overlapping function of three molecular motors: two homologues of the conserved mitotic kinesin-5 family, Cin8 and Kip1, and dynein [4–8]. Kinesin-5 motors, which have been found in numerous eukaryotic species [5, 7, 9–14], play major roles in the assembly of the mitotic spindle, maintenance of its structure before the metaphase to anaphase transition and anaphase spindle elongation [2, 5, 11, 15–18]. These motors have been shown to localize to the spindle midzone [19, 20] and have been suggested to fulfill their mitotic roles by crosslinking and sliding interpolar MTs [21–25]. Cytoplasmic dynein, a minus-end directed motor protein, is located at the cell cortex in the bud and is believed to perform its mitotic roles by applying pulling forces on the spindle via the cytoplasmic MTs [26–28]. Its function has been shown to be essential for mitotic spindle positioning in *S. cerevisiae* cells], as well as in other eukaryotes [29–31].

Among the three molecular motors required for anaphase spindle elongation (Cin8, Kip1 and dynein), dynein has been shown to be synthetically lethal with Cin8 but not with Kip1 [8], indicating that Cin8 and dynein overlap in unique functions that are not shared by dynein and Kip1. However, the overlapping function/s between the cortically-localized dynein and the inner-spindle-localized Cin8 remain/s unclear. This is mainly due to the fact that the arrest phenotype in cells that are eliminated for the function of both Cin8 and dynein has not yet been established.

To reveal the functional overlap between Cin8 and dynein, we studied the phenotypes of cells deleted for the function of dynein and which carry a temperature-sensitive mutation of Cin8 (*cin8-3*), at permissive and non-permissive temperatures. We identified and characterized a unique anaphase arrest phenotype at the non-permissive temperature which is characterized by undivided nuclei barring two MTs asters. We also found that these motors cooperate in midzone organization and that their functional overlap is essential for providing sufficient spindle elongation for nuclear division. Based on these results, we proposed different models that may explain the cooperation between these two motors during anaphase spindle elongation.

Materials and methods

Yeast strains, media and genomic manipulations. The *S. cerevisiae* strains (Table 1) used in this work are derivatives of the S288C strain. Rich (YPD) and minimal (SD) media were described by Sherman et al. [32]. The Cin8 motor domain mutation (*cin8-3*) was described previously [13, 22]. Nuf2-GFP and Tub1-

Table 1. *S. cerevisiae* strains (S288C) used in this study.

Yeast Strains	Genotype
LGY600	<i>a, ura3, leu2, his3, ade2, GAL⁺</i>
LGY322	<i>a, ura3, leu2, his3, ade2, cyh2', dyn1::HIS3, cin8-3</i>
LGY330	<i>a, his3, leu2, lys2, ura3, cyh2', nuf2::NUF2-GFP-URA3</i>
LGY703	<i>a, ura3, ade2, his3, leu2, cin8-3</i>
LGY704	<i>a, ura3, leu2, his3, lys2, cyh2', kip1::HIS3, cin8-3</i>
LGY737	<i>a, ura3, leu2, his3, ade2, dyn1::HIS3</i>
LGY1216	<i>a, ura3, leu2, his3, cyh2', dyn1::HIS3, cin8-3, nuf2::NUF2-GFP-URA3, leu2::LEU2-TUB1-GFP</i>
LGY1218	<i>a, ura3, leu2, his3, ade2, dyn1::HIS3, nuf2::NUF2-GFP-URA3, leu2::LEU2-TUB1-GFP</i>
LGY1480	<i>a, his3, leu2, lys2, ura3, cyh2', nuf2::NUF2-GFP-URA3, leu2::LEU2-TUB1-GFP</i>
LGY1515	<i>a, ura3, leu2, his3, lys2, ade2, cin8-3, nuf2::NUF2-GFP-URA3, leu2::LEU2-TUB1-GFP</i>
LGY1682	<i>a, ura3, leu2, his3, lys2, cyh2', dyn1::LEU2, cin8-3</i>
LGY1683	<i>a, ura3, leu2, his3, lys2, cyh2', dyn1::LEU2, cin8-3, SCC1-GFP::SpHIS5</i>
LGY1726	<i>a, ura3, leu2, his3, lys2, cyh2', dyn1::LEU2, cin8-3, SCC1-GFP::SpHIS5, ura3::URA3-TUB1-GFP</i>
LGY1729	<i>a, ura3, leu2, his3, lys2, cyh2', nuf2::NUF2-GFP-URA3, SCC1-3xHA::SpHIS5</i>
LGY1738	<i>a, ura3, leu2, his3, lys2, cyh2', dyn1::LEU2, cin8-3, nuf2::NUF2-GFP-URA3, SCC1-3xHA::SpHIS5</i>
LGY1828	<i>a, ura3, leu2, his3, lys2, cyh2', dyn1::LEU2, cin8-3, nuf2::NUF2-GFP-URA3, SCC1-GFP::SpHIS5</i>

GFP chromosomal integration was performed as previously described [1]. For Scc1-GFP tagging, first the HIS marker in the LGY322 strain was replaced by the LEU marker using standard techniques. Then, the *SCC1-GFP::HIS3* sequence was amplified by PCR from the YDL003W strain of the yeast GFP fusion clone collection (Invitrogen) and transformed into the LGY1682 strain. Primers for *SCC1-GFP::HIS3* amplification were: 5'-CGTACCAATTGATGCTGGC-TT-3' and 5'-ACCGGTGTACGTGGGCAGAC-3'.

Spindle and nuclear morphologies. Spindle morphologies were visualized by immunostaining of tubulin as previously described [22]. Cell morphologies were visualized by 4,6,-diamidino-2-phenylindole (DAPI, 0.3 µg/mL, Sigma Aldrich) staining. Cells were observed using a fluorescence microscope (see below). In all S-phase arrest and release experiments, cells were grown overnight and back-diluted for 2 h at room temperature. Hydroxyurea (HU, 0.1 M, Sigma Aldrich) was added for synchronization of cells in S-phase, for 3 h at room temperature, washed and resuspended in HU-free medium. In all sorbitol experiments, sorbitol was added to the growth medium to a final concentration of 2 M. Cells were

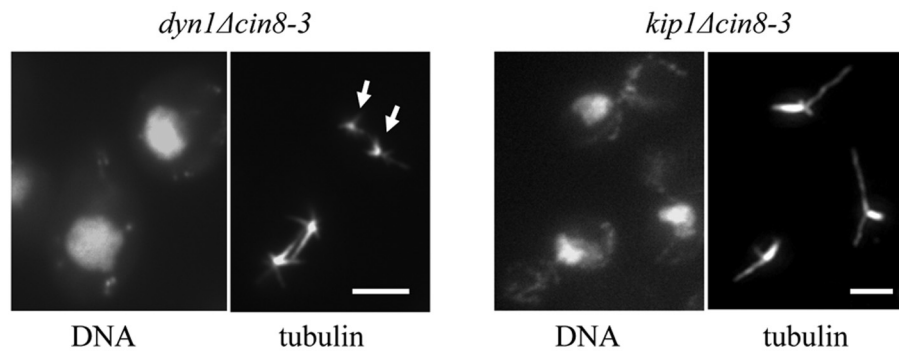


Figure 1. Typical arrest phenotypes of *dyn1Δcin8-3* versus *kip1Δcin8-3* cells at a non-permissive temperature. Cells were arrested for 3 h with HU at room temperature and then incubated at 37°C for 2 h. Left panel: TAN phenotype in *dyn1Δcin8-3* cells – a single nucleus and two separated microtubule asters (designated by arrowheads). Right panel: collapsed monopolar spindles in *kip1Δcin8-3* cells. The field of *dyn1Δcin8-3* TAN cells is presented on a larger scale, to show the details of this phenotype clearly. bar – 2 μm. Strains: LGY 322, 704.

grown overnight, back-diluted for 3 h at room temperature and then shifted to 37°C. Samples were collected at different time points following the shift and analyzed by immunostaining or Western blotting. For synchronization in G1, medium was supplemented with α -factor (5 μg/mL, Sigma Aldrich). To follow spindle morphologies and/or measure spindle length in cells expressing Tub1-GFP, 5 μl of the cells were placed on a microscope slide with an agarose gel layer [1]. The samples were examined on a motorized inverted microscope, Axiovert M200 (Zeiss), on a vibration-isolation table (TMC), supplemented with a cooled CCD camera, SenciCam (PCO) and supported by acquisition and image-processing software, MetaMorph (Universal Imaging). Z-stack images were acquired and the spindle length was measured in 3D, using the MetaMorph or ImageJ softwares.

Western blotting. For protein extract preparation, cells were vortexed with glass beads in 50 mM Tris-HCl (pH = 7.4), 250 mM NaCl, 50 mM NaF, 5 mM EDTA, 1 mM phenylmethylsulfonyl fluoride, for 15 min at 4°C, followed by addition of 2% SDS, boiling for 5 min and centrifugation for 5 min. Supernatants were fractionated on 10% polyacrylamide gel and processed for Western blotting.

Antibodies. The antibodies used for immunostaining included rat anti α -tubulin, 1:400 (YOL1/34, Serotec) and goat anti-rat IgG polyclonal Alexa-Fluor 488 conjugate, 1:500 (Molecular Probes). The antibodies used for Western blotting included rabbit anti-Clb2 polyclonal, 1:500 (Santa Cruz) and goat anti-rabbit IgG HRP conjugated, 1:10000, (W401B, Promega), mouse anti-HA monoclonal, 1:3000 (16B12, Covance) and goat anti-mouse IgG, 1:10000 (W402B, Promega).

Real-time microscopy assay. Cells were grown O/N in liquid minimal medium and back-diluted for 2 h. 5 μl of the cells were placed on a microscope slide with an agarose gel layer (for spatial fixation of the cells) covered with a coverslip. For analysis of cells at 37°C in this method, a heated stage was used. The samples were examined under a Zeiss Axiovert 200M-based Nipkow spinning-disc confocal microscope (Ultra-View ESR, Perkin Elmer, UK) with an EMCCD camera. For measurements of the distance between the spindle pole bodies, Z-stacks images of 0.1–0.2 μm separation between the planes were acquired every minute. The distance between the SPB was measured in 3D, using MetaMorph software.

Results

A unique arrest phenotype in cells eliminated for the function of dynein and Cin8. To study the functional overlap between the kinesin-5 Cin8 and dynein motors, we used cells that carry *DYNI* chromosomal deletion in combination with the temperature-sensitive *cin8-3* mutation [8]. In contrast to the single mutants, the double mutant *dyn1Δcin8-3* cells are not viable at 37°C [8]. Hence, we speculated that the identification and analysis of their death phenotype should help us to reveal the function for which they overlap. For this purpose, we synchronized *dyn1Δcin8-3* cells in S-phase at room temperature, then shifted them to a non-permissive temperature (37°C) and, last, analyzed the nuclei and spindle morphologies by immunostaining. We found that 1–2 h following incubation at the non-permissive temperature, *dyn1Δcin8-3* cells exhibited a unique phenotype characterized by large-budded cells containing a single DNA mass with two separated MT asters (Fig. 1, left). We named this new phenotype TAN

Table 2. Anaphase arrest phenotypes of Cin8 motor domain mutants.

Genotype	Unbudded G1 cells	Budded cells				n ^a
		Mononucleates			Binucleates	
		bipolar spindles	unseparated SPBs ^b	TAN		
WT	22 ± 6	70 ± 4	8 ± 4	< 1	< 1	4
<i>cin8Δ</i>	29 ± 2	45 ± 4	22 ± 3	2 ± 0.3	2 ± 0.3	10
<i>cin8-3</i>	22 ± 4	44 ± 6	27 ± 3	3 ± 0.8	4 ± 1	7
<i>kip1Δ</i>	31 ± 5	61 ± 5	5 ± 1	1 ± 0.5	2 ± 1	5
<i>kip1Δcin8-3</i>	27 ± 4	3 ± 1	70 ± 2	< 1	< 1	5
<i>dyn1Δ</i>	23 ± 4	58 ± 4	3 ± 0.7	5 ± 0.7	15 ± 2	8
<i>dyn1Δcin8-3</i>	26 ± 6	14 ± 5	3 ± 1	45 ± 3	12 ± 3	5
<i>dyn1Δkip1Δ</i>	16 ± 3	50 ± 4	4 ± 1	9 ± 2	18 ± 2	3

Cells were arrested with HU at room temperature and released from arrest to 37°C. 1.5 h following release, cells were processed for immunostaining. In each experiment, 200–300 cells were categorized according to the phenotypes indicated in the top row of the table. Average ± SEM of % from total cells is presented for each strain. The typical death phenotypes of *kip1Δcin8-3* and *dyn1Δcin8-3* cells are marked in bold.

^a – number of experiments for each strain.

^b – monopolar spindles with unseparated spindle pole bodies (SPBs).

(two asters in one nucleus). 1.5 h following the shift to 37°C, this phenotype constituted about 45% of the total cell population (Table 2).

Examination of additional mutants of Cin8, Kip1 and dynein motor proteins, which overlap during anaphase spindle elongation [8], revealed that the TAN phenotype did not appear in either of these mutants (*kip1Δ*, *cin8Δ*, *cin8-3*, *dyn1Δ*, *kip1Δdyn1Δ* and *kip1Δcin8-3*) (Table 2). This finding indicates that the TAN phenotype reflects a loss of the function/s for which Cin8 and dynein uniquely overlap. Although *kip1Δcin8-3* and *dyn1Δcin8-3* cells both lacked intact bipolar spindles at the non-permissive temperature, the TAN phenotype in *dyn1Δcin8-3* cells was different from the typical arrest phenotype of *kip1Δcin8-3* cells (Table 2, in bold). While in *kip1Δcin8-3* cells the spindles appear with unseparated spindle pole bodies (SPBs) ([13], [17] and Fig. 1), in *dyn1Δcin8-3* cells, the spindles decomposed, leaving two separated MT asters (Fig. 1). This difference must be due to the fact that while Cin8 and Kip1 overlap in bipolar spindle assembly and maintenance [6, 7, 13, 17], Cin8 and dynein do not, but rather overlap for a different function during anaphase B.

Cells that are eliminated for the function of Cin8 and dynein arrest in anaphase. To determine whether the TAN cells enter anaphase, despite their lack of intact bipolar spindles, we examined whether Scc1 is cleaved in these cells. Scc1 is a part of the sister chromatid cohesion complex and is cleaved with the onset of anaphase [33]. To follow Scc1 cleavage, cells expressing HA-tagged Scc1 were synchronized in S-phase at room

temperature, shifted to 37°C and processed for Western blot and immunostaining at various time points following the shift. We found that in *dyn1Δcin8-3* cells, Scc1 is cleaved about 45 min following release from a 3 h hydroxyurea (HU) arrest (Fig. 2A), which is comparable to the timing of cleavage in WT cells. Since Western blot analysis represents the protein profile in the total population of cells, while the TAN phenotype is observed only in part of *dyn1Δcin8-3* cell population, we performed experiments to examine Scc1p expression in single cells exhibiting the TAN phenotype. For this purpose, we used real-time GFP imaging in *dyn1Δcin8-3* cells that express Scc1-GFP in combination with Tub1-GFP (to follow spindle morphology) or Nuf2-GFP (to follow the distance between the SPBs). We found that in agreement with previous reports [33, 34], in S-phase arrested cells, Scc1-GFP was spread in the nucleus of cells bearing short spindles (Fig. 2B and C, left). However, 45–90 min following release from HU arrest to 37°C, the Scc1-GFP signal was not observed in the nucleus of cells that exhibit two adjacent Tub1-GFP or Nuf2-GFP spots (Fig. 2B and C, right), indicating that Scc1 is cleaved in these cells [35]. To rule out the possibility that following the shift to 37°C Scc1 relocates to the SPBs, we performed experiments with cells that express Scc1-GFP only (without Tub1-GFP or Nuf2-GFP). Indeed, following the release to 37°C, we did not observe any fluorescence patterns that would indicate re-localization of Scc1 to the SPBs (data not shown). Taken together, these results confirm that the TAN phenotype appears in cells that pass the metaphase to anaphase transition.

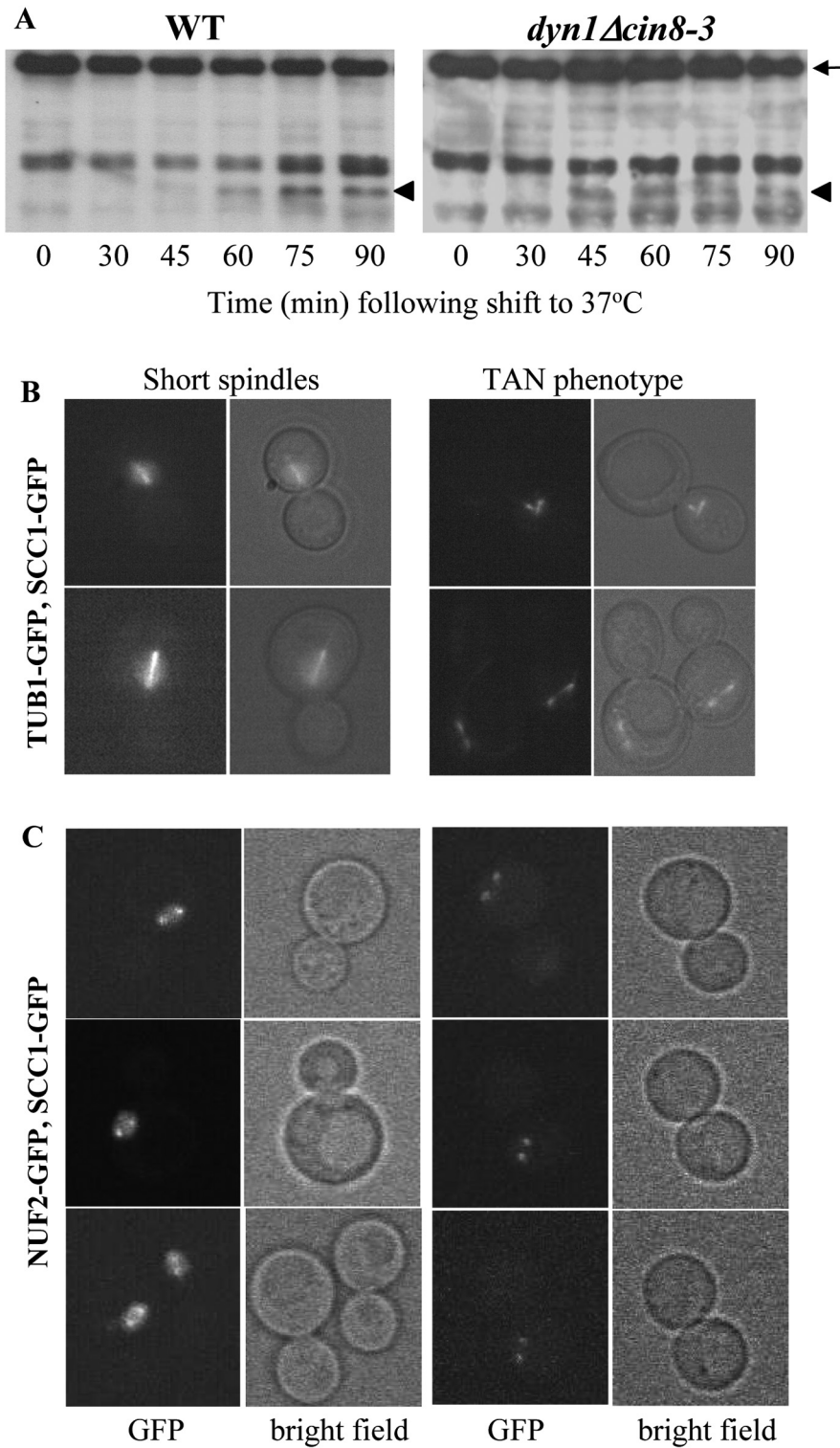









Figure 2 (A) Cleavage of Scc1-3xHA in WT and *dyn1Δcin8-3* cells following incubation at 37°C. Cells were arrested for 3 h with HU at room temperature, shifted to 37°C and then collected at different time points. Cell lysates were analyzed by Western blot for degradation of Scc1-3xHA. Location of the Scc1-3xHA band (~97 kDa) is marked on the right with the top arrow. Scc1-3xHA cleavage product (~50 kDa) is designated by the bottom arrow. Strains: LGY1729, 1738. (B) and (C). Expression of Scc1-GFP in *dyn1Δcin8-3* cells with short spindles versus TAN cells. The Scc1-GFP signal was monitored in *dyn1Δcin8-3* cells with short spindles after 3 h of HU arrest at room temperature and in TAN cells observed 2 h following their shift to 37°C. (B) Cells expressing both Tub1-GFP and Scc1-GFP; (C) Cells expressing both Nuf2-GFP and Scc1-GFP. Strains: LGY1726, 1828.

We next examined whether cells exhibiting the TAN phenotype exit mitosis by analyzing Clb2 levels in WT, *dyn1Δ*, *cin8-3* and *dyn1Δcin8-3* cells at 37°C. Clb2 is the major B-type mitotic cyclin whose levels accumulate from S-phase until late in mitosis [36-38]. To

follow Clb2 levels, cells of mating-type "a" were synchronized in S-phase at room temperature, shifted to 37°C and analyzed for Clb2 levels and cell/DNA morphologies at different time points following the shift (Fig. 3). To prevent cells from entering the next

Table 3. Nuclear morphologies and localization following release from S-phase arrest to 37°C.

							
t = 0^a							
WT	15 ± 2	8 ± 2	61 ± 1	11 ± 2	4 ± 1	0 ± 0	0 ± 0
<i>dyn1Δ</i>	21 ± 3	26 ± 4	48 ± 4	1 ± 0	2 ± 0	1 ± 0	1 ± 1
<i>cin8-3</i>	15 ± 4	14 ± 0	57 ± 2	10 ± 2	4 ± 1	0 ± 0	0 ± 0
<i>dyn1Δcin8-3</i>	12 ± 1	23 ± 2	57 ± 2	3 ± 1	1 ± 0	1 ± 1	3 ± 1
t = 90^a							
WT	59 ± 3	0 ± 0	8 ± 2	1 ± 1	31 ± 4	1 ± 0	0 ± 0
<i>dyn1Δ</i>	48 ± 3	8 ± 2	11 ± 2	1 ± 0	18 ± 2	9 ± 2	5 ± 1
<i>cin8-3</i>	57 ± 3	3 ± 0	12 ± 3	2 ± 0	25 ± 4	0 ± 0	2 ± 1
<i>dyn1Δcin8-3</i>	10 ± 2	33 ± 3	33 ± 2	2 ± 1	8 ± 2	6 ± 1	8 ± 1

Cells were synchronized at S-phase with HU at room temperature and then shifted to 37°C. Cells were then processed for DAPI staining at t = 0, 90 min following the shift. In each experiment, 200–250 cells were categorized according to the phenotypes indicated in the top row of the table. Average ± SEM of % of total cells in three representative experiments is presented for each strain.

^a Time (min) after shift to 37°C

cell cycle, the release medium was supplemented with the yeast pheromone α -factor which induces a G1-arrest with a typical "Shmoo" morphology in cells of mating-type "a" [39, 40]. At t = 0, following release from S-phase arrest, 70–80% of the cells in the different strains were large-budded with a single DNA mass and, as expected, high levels of Clb2 were observed. After 3.5 h of incubation in media supplemented with α -factor at 37°C, ~65% of *dyn1Δ cin8-3* cells were large-budded with a single DNA mass, while only ~20% of *cin8-3* cells and no WT or *dyn1Δ* cells had this morphology. During this period of time, Clb2 levels dropped in WT, *dyn1Δ* and *cin8-3* cells due to their exit of mitosis, while remaining high in *dyn1Δcin8-3* cells (Fig. 3). This result indicates that *dyn1Δcin8-3* cells remain arrested in mitosis for at least 3–4 h following their incubation at the non-permissive temperature.

To understand why *dyn1Δcin8-3* cells do not exit mitosis, we analyzed their nuclei morphologies and localization at t = 0 and t = 1.5 h following release from HU arrest and incubation at 37°C. At t = 0, *dyn1Δcin8-3* cells exhibited a high percentage of mislocalized nuclei, located in the bottom two thirds of the mother cell (Table 3, t = 0). *dyn1Δ* cells exhibited a similar percentage of mislocalized nuclei at this time point (Table 3, t = 0). However, at t = 1.5 h, similarly to WT and *cin8-3* cells, more than 25% of *dyn1Δ* cells had divided their nuclei into two masses, while only 14% had divided their nuclei in *dyn1Δ cin8-3* cells (Table 3, t = 1.5 h). At this time point, more than 70% of *dyn1Δcin8-3* cells were large-budded with a single DNA mass, of which localization

was evenly distributed between the vicinity of the neck and the bottom two thirds of the mother cell (Table 3, t = 1.5 h). Hence, we conclude that the primary cause for the arrest in *dyn1Δcin8-3* cells is their inability to divide their nuclei while the nuclear mislocalization in these cells is the by-product of the arrest.

To further examine whether *dyn1Δcin8-3* cells proceed through cytokinesis, we determined the percentage of large-budded cells with a single DNA mass at periods of time longer than an average cell-cycle (> 2.5–3 h) following release from S-phase arrest and incubation at 37°C. We found that in *dyn1Δcin8-3* cells, the percentage of large-budded cells with a single DNA mass remained almost unchanged for up to 8 h (data not shown), indicating that these cells do not proceed through cytokinesis. Although *cin8-3* cells exhibited a high increase in the percentage of large-budded cells with a single DNA mass after 6–8 h of incubation at 37°C (data not shown), the TAN phenotype was still exclusively exhibited in *dyn1Δ cin8-3* cells. Interestingly, following prolonged incubation at 37°C, a high percentage of *dyn1Δcin8-3* cells rebudded, reaching up to almost 50% compared to only 2–5% of rebudding in *dyn1Δ* or *cin8-3* cells and no rebudding in WT cells. Partial rebudding has also been previously reported in cells that arrest with misaligned spindles due to mutations in dynactin components [41]. Although the mechanism of such partial cell-cycle progression is not clear, it might be a common phenomenon in cells that arrest in anaphase with misaligned spindles.

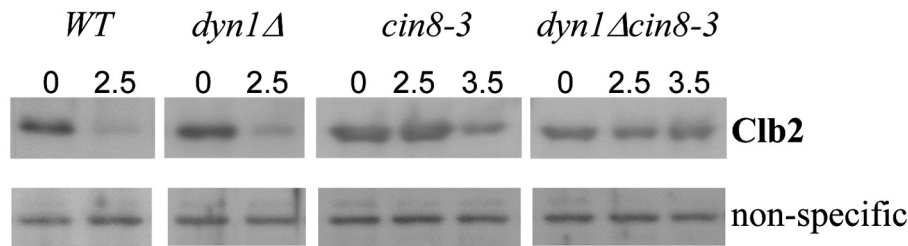


Figure 3. Clb2 levels in WT, *dyn1Δ*, *cin8-3* and *dyn1Δcin8-3* cells after incubation with α -factor at 37°C. Cells were arrested with HU for 3 h at room temperature and then released to YPD media supplemented with 5 μ g/mL α -factor at 37°C. Western blot was carried out for cell-extracts of samples collected at 0, 2.5 and 3.5 h following release. Time (h) of incubation in YPD with α -factor is indicated at the top of the figure. Top panel: Clb2 (55 kDa) levels at the different time points. Bottom panel: levels of a high-molecular weight protein expressed at constant levels as a function of time. The bands of this non-specific protein were used as loading controls. Strains: LGY600, 737, 322, 703.

Elimination of Cin8 and dynein functions prevents progression through the slow phase of anaphase B.

Since we have found that the TAN cells are arrested in anaphase, we further examined anaphase spindle elongation in *dyn1Δcin8-3* cells. First, we performed real-time measurements of anaphase kinetics at a permissive temperature for *dyn1Δcin8-3* cells that express Tub1-GFP together with Nuf2-GFP. Cells were arrested at S-phase for 3 h, released from arrest to fresh liquid medium for 30 min and then placed on a slide with a layer of minimal media agar and analyzed under the microscope. We found that in agreement with previous reports [1, 2], anaphase B spindle elongation of *dyn1Δcin8-3* spindles which are aligned with the mother-bud axis is bi-phasic. However, the rates observed for the fast phase $-0.62 \pm 0.06 \mu\text{m}/\text{min}$ (average \pm SEM, $n = 8$) and for the slow phase $-0.18 \pm 0.02 \mu\text{m}/\text{min}$ (average \pm SEM, $n = 7$) were slower than those reported for WT cells of the same genetic background [42]. Interestingly, these rates were similar to those reported for cells eliminated for the function of kinesin-5 Kip1 combined with a compromised Ase1 activity [42]. Since Ase1 is a major midzone-stabilizing and -organizing protein [3, 43], this result suggests that *dyn1Δcin8-3* cells are compromised for their midzone organization (see below). Real-time measurements, which we carried-out on *dyn1Δcin8-3* cells at 37°C, revealed that cells with short spindles ($\sim 2 \mu\text{m}$) elongated their spindles to a maximal length of 4–5 μm (Fig. 4A). However, irregular fluctuations in spindle length were observed during the elongation of the spindles (Fig. 4A). Because of this irregular elongation, cells remained with intermediate spindles (4–5 μm) for 30–50 min. These spindles eventually shortened to $\sim 2 \mu\text{m}$, leaving two tubulin spots, similar to those observed in the TAN phenotype (Fig. 4A, last two frames). These observations suggest that at the non-permissive temperature, *dyn1Δcin8-3* cells fail to elongate their

spindles to more than 4–5 μm and that the TAN phenotype is an outcome of this defect.

To validate our real-time observations, we followed the changes in spindle morphologies in large populations of fixed cells. *dyn1Δcin8-3*, *dyn1Δ* and *cin8-3* cells were arrested in S-phase at room temperature, shifted to 37°C and analyzed by immunostaining for their spindle morphologies at different time points following the shift. At $t = 0$, 70–85% of the cells exhibited short ($< 2 \mu\text{m}$) spindles (Fig. 4B, $t = 0$). After 30–60 minutes of incubation at 37°C, cells of all strains exhibited anaphase spindles longer than 2 μm , although elongated spindles in *dyn1Δcin8-3* cells seemed shorter than those in the other cells (Fig. 4B, $t = 45$). Measurements of spindle length at different time points between 30–120 min following release of cells from HU arrest confirmed that the average length of elongated spindles ($> 2 \mu\text{m}$) was significantly shorter in *dyn1Δcin8-3* cells. The average length of elongated spindles measured for the different strains was as follows: WT – $5.7 \pm 1.7 \mu\text{m}$, *cin8-3* – $5.2 \pm 1.5 \mu\text{m}$, *dyn1Δ* – $5.4 \pm 1.5 \mu\text{m}$ and *dyn1Δcin8-3* – $3.7 \pm 0.77 \mu\text{m}$ (average \pm SD of at least 100 spindles). 90 min following the shift to 37°C, about 45% of *dyn1Δcin8-3* cells exhibited the TAN phenotype, while *dyn1Δ* or *cin8-3* cells exhibited either G1, collapsed or bipolar spindles (Fig. 4B, $t = 90$, Table 2). An analysis of the maximal length of spindles obtained in each of the examined strains revealed that in *dyn1Δcin8-3* cells only 4% of the elongated spindles were longer than 5 μm as compared to 50%, or more, in *dyn1Δ* or *cin8-3* single mutant cells (Fig. 4C). The finding that the maximal spindle length in *dyn1Δcin8-3* cells at 37°C is 5 μm indicates that the functional overlap between Cin8 and dynein affects the progression of the slow phase of anaphase B, at which the spindles elongate from 4–5 to 8–10 μm [1].

Combined mutations in Cin8 and dynein affect spindle rigidity. To study the possible correlation between the

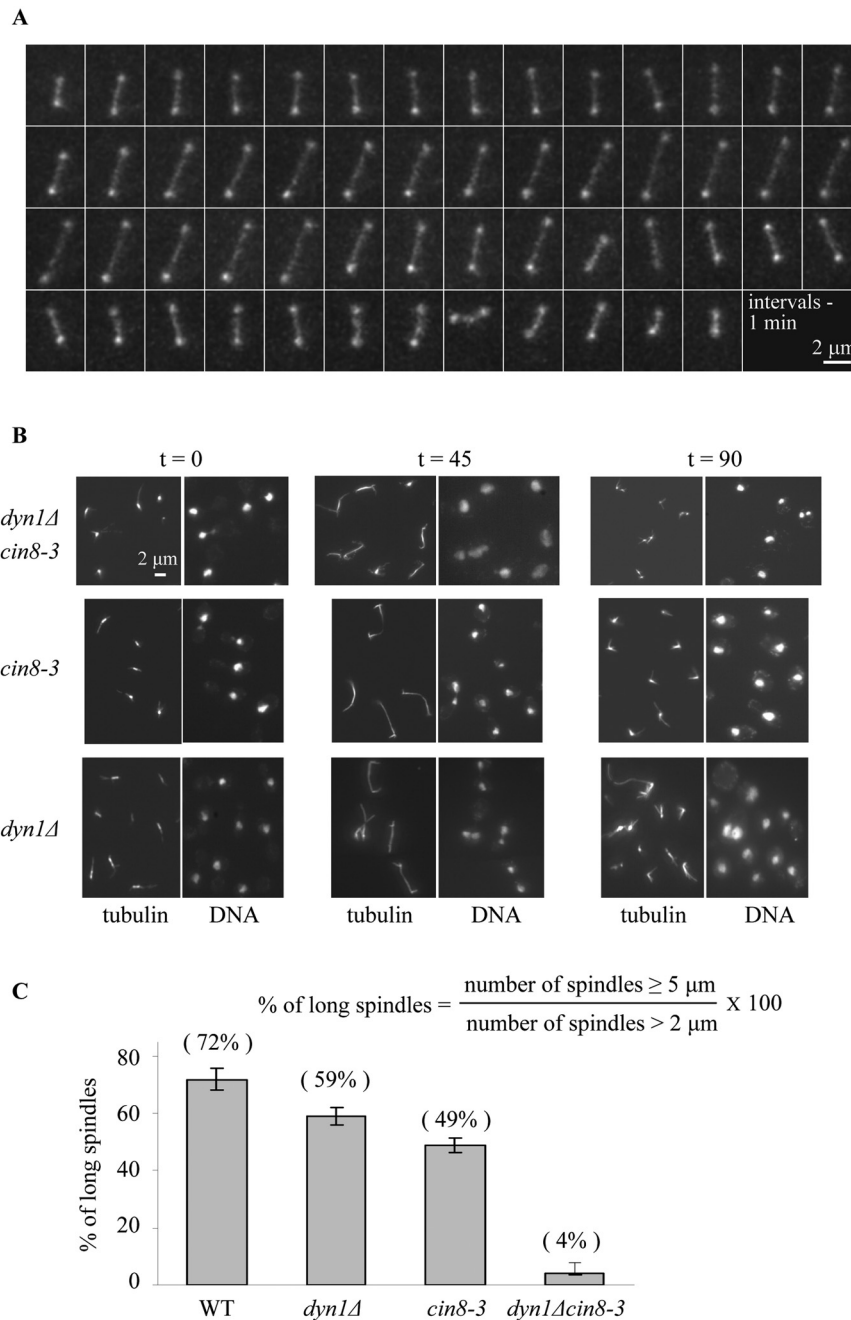


Figure 4. Spindle elongation at the non-permissive temperature. (A) Real-time imaging of *dyn1Δ cin8-3* cells at 37°C. *dyn1Δcin8-3* cells that express Tub1-GFP and Nuf2-GFP were grown overnight at room temperature. Cells were then placed on a microscope slide with a minimal medium agarose gel layer. During the analysis, the slide was placed on a stage heated to 37°C. The sequence is representative of 8 cells. Strain: LGY1216. (B) Analysis of fixed cells. *dyn1Δ, cin8-3* and *dyn1Δcin8-3* cells were arrested in S-phase at room temperature and shifted to 37°C. Immunostaining was carried out for samples collected 0, 45 and 90 min following the shift. Representative fields of spindles and nuclei morphologies at the different time points are shown. Bar – 2 μm. Strains: LGY737, 322, 703. (C) *dyn1Δcin8-3* cells fail to elongate spindles to more than 5 μm. The length of 100–150 elongated spindles (> 2 μm) was measured for each of the above strains at several time points between 30–120 min following a shift to 37°C. Spindle length was measured with the ImageJ software.

failure of *dyn1Δcin8-3* cells to elongate spindles above 5 μm and the lack of DNA division in these cells at 37°C (Table 3), we determined the length of spindles required for DNA division at room temperature. We found that in all strains, when spindles were shorter than 4.5 μm, the majority of cells contained only one non-divided DNA mass (Fig. 5). However, when the spindle length reached 5.5–6 μm, about 80% of WT, *dyn1Δ* and *cin8-3* cells had two DNA masses, compared to only 46% of *dyn1Δcin8-3* cells (Fig. 5). We conclude that in *dyn1Δcin8-3* cells at

the non-permissive temperature, the failure to elongate the spindle above 5 μm (Fig. 4C) may be the main cause for their inability to divide their nucleus. Furthermore, our finding that *dyn1Δcin8-3* cells with long anaphase spindles (> 5 μm) exhibit a comparatively low percentage of divided DNA masses (Fig. 5) suggests that the rigidity of these spindles is compromised and insufficient for nuclear division. To determine whether the rigidity of anaphase spindles is indeed affected by mutations in Cin8 and dynein, we analyzed spindle morphologies at room

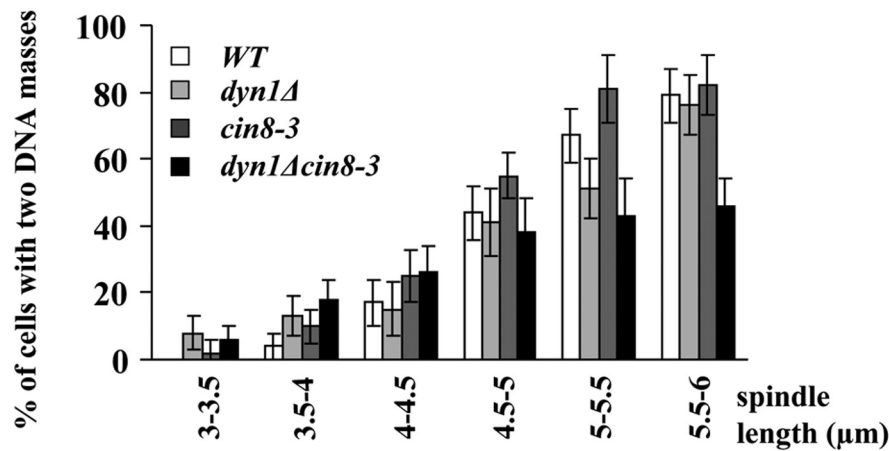


Figure 5. Percentage of cells with two DNA masses as a function of spindle length. Cells were grown overnight at room temperature, processed for DAPI and tubulin staining and categorized according to their spindle length (indicated in the bottom). Columns and bars represent average \pm SEM of two representative experiments. The different genotypes are indicated: WT – white, *dyn1Δ* – light gray, *cin8-3* – dark gray, *dyn1Δcin8-3* – black. In each experiment, 30–50 cells were counted for each genotype and each range of length. Strains: LGY600, 737, 322, 703.

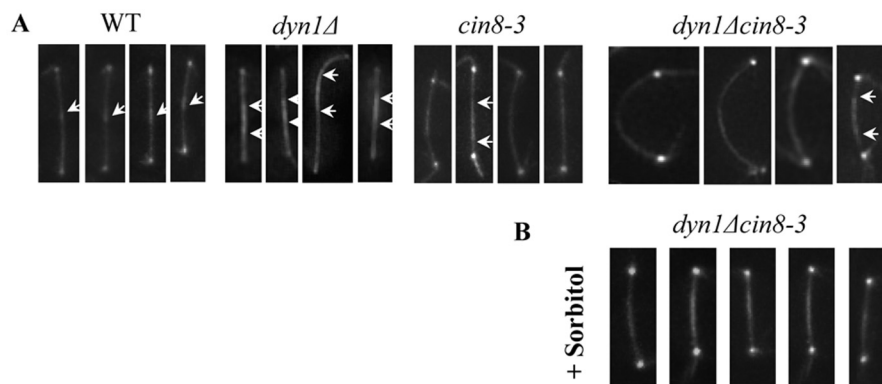


Figure 6. (A) Dynein and Cin8 affect the morphology of the spindle midzone. WT, *dyn1Δ*, *cin8-3* and *dyn1Δcin8-3* cells expressing Tub1-GFP and Nuf2-GFP fusion proteins were grown overnight at room temperature. Cells were then analyzed for their anaphase spindle morphologies. Representative images of three experiments are shown. The genotype of the cells is assigned at the top of the figure. The midzone (the brighter region of the overlapping antiparallel interpolar MTs in the middle of the spindle) or the borders of the midzone are designated by arrowheads. Strains: LGY1216, 1218, 1480, 1515. (B) Sorbitol increases the rigidity of anaphase spindles in *dyn1Δcin8-3* cells. The growth medium of *dyn1Δcin8-3* cells grown overnight was supplemented with 2 M sorbitol. 12 h following the addition of sorbitol, cells were analyzed for their anaphase spindle morphologies. Representative images of three experiments are shown. Bar – 2 μ m. Strain: LGY1216.

temperature in *dyn1Δcin8-3*, WT, *dyn1Δ* and *cin8-3* cells that express Nuf2-GFP and Tub1-GFP. Using real-time microscopy, we found that the cells of these strains differed in the morphology and/or in the midzone size of their long anaphase spindles ($>5 \mu$ m). In WT cells, long spindles contained a well-defined midzone, which accounted for $15.0\% \pm 4.4\%$ (average \pm SD, $n = 24$) of the spindle length (Fig. 6A, arrowhead). However, *dyn1Δ* long spindles contained a significantly larger midzone (Fig. 6A, arrowhead), which accounted for $23.5\% \pm 7.4\%$ (average \pm SD, $n = 23$) of the spindle length. In most of *cin8-3* cells, the midzone was either non-detectable or diffusive along the long spindles (Fig. 6A) and in *dyn1Δcin8-3* cells, more than 50% of the long spindles were extremely bent and flexible and had either a non-detectable midzone or a diffusive one (Fig. 6A). These

findings indicate that mutations in Cin8 and dynein perturb the rigidity of anaphase spindles and their midzone morphology at the permissive temperature. We further suggest that the disassembly of the spindles in TAN cells at the non-permissive temperature is due to the enhancement of these defects.

Sorbitol suppresses the TAN phenotype in *dyn1Δcin8-3* cells. To explore the possibility that the appearance of the TAN phenotype in *dyn1Δcin8-3* cells is correlated to their defects in spindle rigidity, we analyzed the effect of sorbitol on these cells at permissive and non-permissive temperatures. Addition of sorbitol to the growth medium has been previously shown to suppress sensitivity to the MT-depolymerizing agent, benomyl, [44], suggesting that sorbitol induces MT stabilization. Sorbitol has also been

shown to rescue the viability of *dyn1Δcin8-3* cells at a non-permissive temperature [44]. Therefore, examination of its influence on the morphology of anaphase spindles at the permissive temperature – on the one hand – and on the appearance of TAN cells at the non-permissive temperature – on the other – may shed light on the correlation between the two phenotypes.

For the following experiments with sorbitol, we first determined the doubling times of cells grown with sorbitol (2 M) and found that they were ~2–3 folds longer than without sorbitol (YPD with sorbitol: WT – 7.2 h, *dyn1Δ* – 6.8 h, *cin8-3* – 5.2 h, *dyn1Δcin8-3* – 7.2 h; without sorbitol: WT – 2.5 h, *dyn1Δ* – 3.1 h, *cin8-3* – 2.9 h, *dyn1Δcin8-3* – 3.0 h). Then, we analyzed spindle morphologies at a time point corresponding to about one doubling time following a temperature shift to 37°C (3 h in medium lacking sorbitol and 7.5 h in medium containing sorbitol). Due to the long doubling-time in the presence of sorbitol, synchronization in S-phase was not efficient and hence we performed the temperature shift in unsynchronized cultures. We observed a lower percentage of the TAN morphology compared to experiments with synchronized cultures. However, the percentage of TAN cells of total large-budded cells with a single DNA mass dropped by 2.5 fold in the presence of sorbitol (12% with sorbitol versus 31% without sorbitol). This result clearly indicates that sorbitol suppresses the TAN phenotype. We also found that at a permissive temperature, sorbitol eliminated the appearance of bent anaphase spindles in *dyn1Δcin8-3* cells that express Nuf2-GFP and Tub1-GFP (Fig. 6A). In the presence of sorbitol, spindles were straighter and considerably brighter (Fig. 6A and B) than spindles of cells grown without sorbitol. Hence, our results clearly show that the appearance of the TAN phenotype in *dyn1Δcin8-3* cells is correlated to the defects in spindle rigidity in these cells.

We further analyzed localization of nuclei stained by DAPI at different time points between 0–10 h following a temperature shift to 37°C in YPD medium, with and without sorbitol. At $t = 0$, about 25% of the nuclei of the large-budded cells with a single DNA mass were mislocalized (Tables 3 and 4). 4 h following incubation at 37°C in YPD, a time that is equivalent to $\sim 1\frac{1}{3}$ cell-cycle, the percentage of mislocalized nuclei in large-budded cells with a single DNA mass increased to about 65%. However, in the presence of sorbitol, at a time equivalent to $\sim 1\frac{1}{3}$ cell-cycle (10 h), the percentage of mislocalized nuclei increased to only 35% (Table 4). Furthermore, while in the absence of sorbitol the percentage of extra-budded cells increased from 3% to 48% during this course of time, only 9% of extra-budded cells were observed in the presence of sorbitol. Taken together, our results indicate that sorbitol

suppresses the TAN phenotype and rescues the viability of *dyn1Δcin8-3* cells by increasing the rigidity of spindles and by correcting defects in nuclear localization in these cells at the non-permissive temperature.

Table 4. Percentage of mislocalized undivided nuclei in *dyn1Δcin8-3* cells +/- sorbitol.

Time following shift to 37°C (h)	% of mislocalized undivided nuclei	
	YPD	YPD + sorbitol
0	26 ± 3	26 ± 3
1.5	41 ± 4	23 ± 8
2.0	41 ± 5	29 ± 7
2.5	40 ± 5	15 ± 3
3.5	48 ± 8 ^a	17 ± 7
4.0	66 ± 14 ^a	27 ± 5
5.0	nd	28 ± 7
10	nd	35 ± 5

WT cells were grown overnight at room temperature and shifted to 37°C, with or without the addition of 2 M sorbitol to the YPD medium. Cells were processed for DAPI staining at different time points following the shift. Localization of the DNA mass was analyzed in 200–250 cells at each time point. Average ± SEM of % of total large-budded cells with a single DNA mass in two representative experiments is presented for each strain.

^a More than two thirds of cells are extra-budded.

Discussion

The results presented in this study show that anaphase B progression is disturbed in *S. cerevisiae* cells that are eliminated for the function of both Cin8 and dynein motor proteins. This disruption is reflected in the new phenotype that we revealed for *dyn1Δcin8-3* cells at the non-permissive temperature, the TAN phenotype, characterized by large-budded cells bearing a single nucleus with two MT asters. Numerous factors which interfere with anaphase B progression have been previously reported. These include mutations in motor proteins that slow spindle elongation rates [2]; mutations in the dynein/dynactin complex or in cortical attachment of the cytoplasmic MTs in the bud which affect spindle positioning and orientation [41, 45–48] and DNA damage occurring during the course of anaphase [49]. In the majority of these cases, cells did not arrest in anaphase but rather the completion of anaphase was delayed and eventually achieved when one of the SPBs translocated to the daughter cell [50–54] and activated the mitotic exit network [55–57]. However, here we show that when the function of both Cin8 and dynein is eliminated, nuclear division and, thus, the translocation of a SPB into the bud are prevented. As a result of this, the

mitotic exit network cannot be activated and cells remain arrested at anaphase [58]).

Cin8 and dynein have been shown to be synthetically lethal and to cooperate during anaphase spindle elongation [4–8]. However, the nature of their cooperation was unclear. Here we demonstrate that Cin8 and dynein are required for progression through the slow phase of anaphase B, since elimination of their function results in the inability of cells to elongate the spindles above 5 μm leading to a mid-anaphase arrest. We also demonstrate that at the permissive temperature, either mutation in Cin8 (*cin8-3*) or chromosomal deletion of dynein affect the morphology of the spindle midzone. In the double mutant cells, *dyn1 Δ cin8-3*, not only the midzone is disrupted but the spindles are profoundly bent and non-rigid. These defects seem to be exacerbated at the restrictive temperature, which leads to the lack of nuclear division and spindle disassembly in the TAN cells. Sorbitol, which has been previously suggested to support MT stabilization [44], increases the rigidity of *dyn1 Δ cin8-3* spindles at the permissive temperature and suppresses their breakdown at the restrictive temperature. Based on these findings, we suggest that the failure of *dyn1 Δ cin8-3* cells to proceed through mid to late anaphase at the non-permissive temperature is an outcome of defects in midzone organization and perturbed MT dynamics. These defects prevent from *dyn1 Δ cin8-3* cells from elongating their spindles sufficiently for nuclear division, thereby leading to their arrest at mid-anaphase as large-budded cells with a single DNA mass. The idea that Cin8 and dynein may cooperate in the organization of the spindle midzone and the control of MT dynamics is supported by the previously reported finding that in the absence of *S. cerevisiae* Ase1, a major mitotic spindle midzone stabilizing protein [59], spindles collapse at mid-anaphase and cells do not proceed through the slow phase of anaphase B [3]. Further support to this idea arises from our real-time measurements, which show that the rate of spindle elongation in *dyn1 Δ cin8-3* cells is similar to that in cells which have a compromised activity of Ase1 in combination with kinesin-5 *kip1* deletion [42].

Three possible models can be proposed to explain the cooperation between Cin8 and dynein. In the first, both motors directly associate with MTs at the midzone and their absence therefore disrupts midzone organization. Previous reports regarding the functions of kinesin-related motor proteins in midzone and spindle MT organization [19, 60–64] as well as in control of MT dynamics [65–69] support this idea. In addition, we have recently reported that a combination of mutations in kinesin-5 motors disrupts midzone organization and centering [42]. An additional

line of evidence that supports this model is that proteins that associate with dynein have been shown to localize at the midzone in several eukaryotic organisms [70, 71]. However, this suggested model is less likely in *S. cerevisiae* cells, since thus far, localization of dynein or dynein-associated proteins to the midzone has not been demonstrated.

In the second model, Cin8 directly affects MT dynamics at the midzone, as suggested in the first model, but the effect of the cortical dynein is indirect. In support of this model, it has been reported that in *Drosophila* cells, the dynein-dynactin complex facilitates the recruitment of factors that are involved in central spindle organization [72] and proteins that associate with dynein have been shown to be involved in MT organization at the midzone [73]. The plausibility of such cooperation between an inner-spindle-localized protein and a cortically-localized one is also supported by a growing body of evidence for interplay between the central spindle and cell cortex during anaphase, in high eukaryote as well as in *S. cerevisiae* cells [19, 74–79]. In this type of model, the cooperation between the inner-spindle Cin8 and the cortical dynein may involve, for example, a biochemical signaling similar to the one reported in HeLa cells, where an intracellular phosphorylation gradient was shown to be produced following the activation of Aurora B kinase, thereby allowing signaling from the midzone to the cell cortex [80].

In the third model, we suggest that the cooperation of Cin8 and dynein motor proteins results from the generation of a delicate balance of counteracting pushing and pulling forces on the anaphase spindles [81]. While Cin8 exerts pushing forces from inside the midzone [13, 17], dynein exerts pulling forces through the cytoplasmic MTs [26, 28, 45, 82]. When the function of either of the motors is weakened/eliminated, this balance is disturbed, accounting for the perturbed midzone morphology that we observe. This perturbation might further induce changes in the tension along the spindle and re-distribution of midzone associated proteins. As a result, at mid-anaphase, the midzone in these cells is structurally weakened, ultimately leading to the disassembly of spindles and to the death of these cells.

Acknowledgments. This work was supported in part by the Israel-US Bi-National grant no. 2003141 awarded to L. G. and M. A. H and the Israel Science Foundation grant no. 822/04 awarded to L. G.

- 1 Kahana, J. A., Schnapp, B. J. and Silver, P. A. (1995). Kinetics of spindle pole body separation in budding yeast. *Proc. Natl. Acad. Sci. USA* 92, 9707–9711.
- 2 Straight, A. F., Sedat, J. W. and Murray, A. W. (1998). Time-lapse microscopy reveals unique roles for kinesins during anaphase in budding yeast. *J. Cell Biol.* 143, 687–694.

- 3 Schuyler, S. C., Liu, J. Y. and Pellman, D. (2003). The molecular function of Ase1p: evidence for a MAP-dependent midzone-specific spindle matrix. *Microtubule-associated proteins*. *J. Cell Biol.* 160, 517–28.
- 4 Geiser, J. R., Schott, E. J., Kingsbury, T. J., Cole, N. B., Totis, L. J., Bhattacharyya, G., He, L. and Hoyt, M. A. (1997). *Saccharomyces cerevisiae* genes required in the absence of the CIN8-encoded spindle motor act in functionally diverse mitotic pathways. *Mol. Biol. Cell* 8, 1035–1050.
- 5 Heck, M. M., Pereira, A., Pesavento, P., Yannoni, Y., Spradling, A. C. and Goldstein, L. S. (1993). The kinesin-like protein KLP61F is essential for mitosis in *Drosophila*. *J. Cell Biol.* 123, 665–679.
- 6 Hoyt, M. A. and Geiser, J. R. (1996). Genetic analysis of the mitotic spindle. *Annu. Rev. Genet.* 30, 7–33.
- 7 Roof, D. M., Meluh, P. B. and Rose, M. D. (1992). Kinesin-related proteins required for assembly of the mitotic spindle. *J. Cell Biol.* 118, 95–108.
- 8 Saunders, W. S., Koshland, D., Eshel, D., Gibbons, I. R. and Hoyt, M. A. (1995). *Saccharomyces cerevisiae* kinesin- and dynein-related proteins required for anaphase chromosome segregation. *J. Cell Biol.* 128, 617–624.
- 9 Asada, T., Kuriyama, R. and Shibaoka, H. (1997). TKRP125, a kinesin-related protein involved in the centrosome-independent organization of the cytokinetic apparatus in tobacco BY-2 cells. *J. Cell Sci.* 110, 179–89.
- 10 Blangy, A., Lane, H. A., d'Herin, P., Harper, M., Kress, M. and Nigg, E. A. (1995). Phosphorylation by p34cdc2 regulates spindle association of human Eg5, a kinesin-related motor essential for bipolar spindle formation in vivo. *Cell* 83, 1159–1169.
- 11 Enos, A. P. and Morris, N. R. (1990). Mutation of a gene that encodes a kinesin-like protein blocks nuclear division in *A. nidulans*. *Cell* 60, 1019–1027.
- 12 Hagan, I. and Yanagida, M. (1992). Kinesin-related cut7 protein associates with mitotic and meiotic spindles in fission yeast. *Nature* 356, 74–6
- 13 Hoyt, M. A., He, L., Loo, K. K. and Saunders, W. S. (1992). Two *Saccharomyces cerevisiae* kinesin-related gene products required for mitotic spindle assembly. *J. Cell Biol.* 118, 109–120.
- 14 Le Guellec, R., Paris, J., Couturier, A., Roghi, C. and Philippe, M. (1991). Cloning by differential screening of a *Xenopus* cDNA that encodes a kinesin-related protein. *Mol. Cell Biol.* 11, 3395–3398.
- 15 Cole, D. G., Saxton, W. M., Sheehan, K. B. and Scholey, J. M. (1994). A "slow" homotetrameric kinesin-related motor protein purified from *Drosophila* embryos. *J. Biol. Chem.* 269, 22913–22916.
- 16 Cottingham, F. R., Gheber, L., Miller, D. L. and Hoyt, M. A. (1999). Novel roles for *saccharomyces cerevisiae* mitotic spindle motors. *J. Cell Biol.* 147, 335–350.
- 17 Saunders, W. S. and Hoyt, M. A. (1992). Kinesin-related proteins required for structural integrity of the mitotic spindle. *Cell* 70, 451–458.
- 18 Sawin, K. E., LeGuellec, K., Philippe, M. and Mitchison, T. J. (1992). Mitotic spindle organization by a plus-end-directed microtubule motor. *Nature* 359, 540–543.
- 19 Raich, W. B., Moran, A. N., Rothman, J. H. and Hardin, J. (1998). Cytokinesis and midzone microtubule organization in *Caenorhabditis elegans* require the kinesin-like protein ZEN-4. *Mol. Biol. Cell* 9, 2037–49.
- 20 Tytell, J. D. and Sorger, P. K. (2006). Analysis of kinesin motor function at budding yeast kinetochores. *J. Cell Biol.* 172, 861–74.
- 21 Barton, N.R. and Goldstein, L.S. (1996). Going mobile: microtubule motors and chromosome segregation. *Proc. Natl. Acad. Sci. USA* 93, 1735–42.
- 22 Gheber, L., Kuo, S. C. and Hoyt, M. A. (1999). Motile properties of the kinesin-related Cin8p spindle motor extracted from *Saccharomyces cerevisiae* cells. *J. Biol. Chem.* 274, 9564–9572.
- 23 Kapoor, T. M. and Mitchison, T. J. (2001). Eg5 is static in bipolar spindles relative to tubulin: evidence for a static spindle matrix. *J. Cell Biol.* 154, 1125–1133.
- 24 Kashina, A. S., Baskin, R. J., Cole, D. G., Wedaman, K.P., Saxton, W.M. and Scholey, J. M. (1996). A bipolar kinesin. *Nature* 379, 270–272.
- 25 Sharp, D. J., McDonald, K. L., Brown, H. M., Matthies, H. J., Walczak, C., Vale, R. D., Mitchison, T. J. and Scholey, J. M. (1999). The bipolar kinesin, KLP61F, cross-links microtubules within inter-polar microtubule bundles of *Drosophila* embryonic mitotic spindles. *J. Cell Biol.* 144, 125–138.
- 26 Eshel, D., Urrestarazu, L. A., Vissers, S., Jauniaux, J. C., van Vliet-Reedijk, J. C., Planta, R.J. and Gibbons, I.R. (1993). Cytoplasmic dynein is required for normal nuclear segregation in yeast. *Proc. Natl. Acad. Sci. USA* 90, 11172–11176.
- 27 Li, Y. Y., Yeh, E., Hays, T. and Bloom, K. (1993). Disruption of mitotic spindle orientation in a yeast dynein mutant. *Proc. Natl. Acad. Sci. USA* 90, 10096–10100.
- 28 Yeh, E., Skibbens, R. V., Cheng, J. W., Salmon, E. D. and Bloom, K. (1995). Spindle dynamics and cell cycle regulation of dynein in the budding yeast, *Saccharomyces cerevisiae*. *J. Cell Biol.* 130, 687–700.
- 29 Fink, G. R., Schuchardt, I., Colombelli, J., Stelzer, E. and Steinberg, G. (2006). Dynein-mediated pulling forces drive rapid mitotic spindle elongation in *Ustilago maydis*. *EMBO J.* 25, 4897–4808.
- 30 Gonczy, P., Pichler, S., Kirkham, M. and Hyman, A. A. (1999). Cytoplasmic dynein is required for distinct aspects of MTOC positioning, including centrosome separation, in the one cell stage *Caenorhabditis elegans* embryo. *J. Cell Biol.* 147, 135–50.
- 31 Vaisberg, E. A., Koonce, M. P. and McIntosh, J. R. (1993). Cytoplasmic dynein plays a role in mammalian mitotic spindle formation. *J. Cell Biol.* 123, 849–58.
- 32 Sherman, F., Fink, G. R. and Hicks, J. B. (1983). *Methods in Yeast Genetics*.
- 33 Uhlmann, F., Lottspeich, F. and Nasmyth, K. (1999). Sister-chromatid separation at anaphase onset is promoted by cleavage of the cohesin subunit Scc1. *Nature* 400, 37–42.
- 34 Shimada, K. and Gasser, S. M. (2007). The origin recognition complex functions in sister-chromatid cohesion in *Saccharomyces cerevisiae*. *Cell* 128, 85–99.
- 35 Gruber, S., Haering, C. and Nasmyth, K. (2003). Chromosomal Cohesion Forms a Ring. *Cell* 112, 765–777.
- 36 Dahmann, C. and Futcher, B. (1995). Specialization of B-type cyclins for mitosis or meiosis in *S. cerevisiae*. *Genetics* 140, 957–963.
- 37 Grandin, N. and Reed, S. I. (1993). Differential function and expression of *Saccharomyces cerevisiae* B-type cyclins in mitosis and meiosis. *Mol. Cell Biol.* 13, 2113–2125.
- 38 Richardson, H., Lew, D. J., Henze, M., Sugimoto, K. and Reed, S. I. (1992). Cyclin-B homologs in *Saccharomyces cerevisiae* function in S phase and in G2. *Genes Dev.* 6, 2021–2034.
- 39 Chan, R. K. and Otte, C. A. (1982). Isolation and genetic analysis of *Saccharomyces cerevisiae* mutants supersensitive to G1 arrest by a factor and alpha factor pheromones. *Mol. Cell Biol.* 2, 11–20.
- 40 Liao, H. and Thorner, J. (1980). Yeast mating pheromone alpha factor inhibits adenylate cyclase. *Proc. Natl. Acad. Sci. USA* 77, 1898–1902.
- 41 Kahana, J. A., Schlenstedt, G., Evanchuk, D. M., Geiser, J. R., Hoyt, M. A. and Silver, P. A. (1998). The yeast dynactin complex is involved in partitioning the mitotic spindle between mother and daughter cells during anaphase B. *Mol. Biol. Cell* 9, 1741–1756.
- 42 Movshovich, N., Fridman, V., Gerson-Gurwitz, A., Shumacher, I., Gertsberg, I., Fich, A., Hoyt, M. A., Katz, B. and Gheber, L. (2008). Slk19-dependent mid-anaphase pause in kinesin-5-mutated cells. *J. Cell Sci.* 121, 2529–39.
- 43 Khmelinskii, A., Lawrence, C., Roostalu, J. and Schiebel, E. (2007). Cdc14-regulated midzone assembly controls anaphase B. *J. Cell Biol.* 177, 981–93.

- 44 Korolyev, E., Steinberg-Neifach, O. and Eshel, D. (2005). Mutations in the yeast kinesin-like Cin8p are alleviated by osmotic support. *FEMS Microbiol. Lett.* 244, 379–83.
- 45 Carminati, J. L. and Stearns, T. (1997). Microtubules orient the mitotic spindle in yeast through dynein-dependent interactions with the cell cortex. *J. Cell Biol.* 138, 629–641.
- 46 Clark, S. W. and Meyer, D. I. (1994). ACT3: a putative centractin homologue in *S. cerevisiae* is required for proper orientation of the mitotic spindle. *J. Cell Biol.* 127, 129–138.
- 47 McMillan, J. N. and Tatchell, K. (1994). The JNM1 gene in the yeast *Saccharomyces cerevisiae* is required for nuclear migration and spindle orientation during the mitotic cell cycle. *J. Cell Biol.* 125, 143–158.
- 48 Muhua, L., Karpova, T. S. and Cooper, J. A. (1994). A yeast actin-related protein homologous to that in vertebrate dynactin complex is important for spindle orientation and nuclear migration. *Cell* 78, 669–79.
- 49 Yang, S. S., Yeh, E., Salmon, E. D. and Bloom, K. (1997). Identification of a mid-anaphase checkpoint in budding yeast. *J. Cell Biol.* 136, 345–54.
- 50 Bardin, A. J., Visintin, R. and Amon, A. (2000). A mechanism for coupling exit from mitosis to partitioning of the nucleus. *Cell* 102, 21–31.
- 51 Bloecher, A., Venturi, G. M. and Tatchell, K. (2000). Anaphase spindle position is monitored by the BUB2 checkpoint. *Nat. Cell Biol.* 2, 556–8.
- 52 Bloom, G. S. and Endow, S. A. (1995). Motor proteins 1: kinesins. *Protein Profile* 2, 1105–1171.
- 53 Hoyt, M. A. (2000). Exit from Mitosis: Spindle Pole Power. *Cell* 102, 267–270.
- 54 Pereira, G., Höfken, T., Grindlay, J., Manson, C. and Schiebel, E. (2000). The Bub2p Spindle Checkpoint Links Nuclear Migration with Mitotic Exit. *Molecular Cell* 6, 1–10.
- 55 Piatti, S., Venturetti, M., Chirotti, E. and Fraschini, R. (2006). The spindle position checkpoint in budding yeast: the motherly care of MEN. *Cell Div.* 1, 2.
- 56 Stegmeier, F. and Amon, A. (2004). Closing mitosis: the functions of the Cdc14 phosphatase and its regulation. *Annu. Rev. Genet.* 38, 203–32.
- 57 Tan, A. L., Rida, P. C. and Surana, U. (2005). Essential tension and constructive destruction: the spindle checkpoint and its regulatory links with mitotic exit. *Biochem. J.* 386, 1–13.
- 58 Lew, D. J. and Burke, D. J. (2003). The spindle assembly and spindle position checkpoints. *Annu. Rev. Genet.* 37, 251–82.
- 59 Pellman, D., Bagget, M., Tu, Y. H., Fink, G. R. and Tu, H. (1995). Two microtubule-associated proteins required for anaphase spindle movement in *Saccharomyces cerevisiae*. *J. Cell Biol.* 130, 1373–1385.
- 60 Adams, R. R., Tavares, A. A., Salzberg, A., Bellen, H. J. and Glover, D. M. (1998). pavarotti encodes a kinesin-like protein required to organize the central spindle and contractile ring for cytokinesis. *Genes Dev.* 12, 1483–94.
- 61 Cesario, J. M., Jang, J. K., Redding, B., Shah, N., Rahman, T. and McKim, K. S. (2006). Kinesin 6 family member Subito participates in mitotic spindle assembly and interacts with mitotic regulators. *J. Cell Sci.* 119, 4770–80.
- 62 Konzack, S., Rischitor, P. E., Enke, C. and Fischer, R. (2005). The role of the kinesin motor KipA in microtubule organization and polarized growth of *Aspergillus nidulans*. *Mol. Biol. Cell* 16, 497–506.
- 63 Kurasawa, Y., Earnshaw, W. C., Mochizuki, Y., Dohmae, N. and Todokoro, K. (2004). Essential roles of KIF4 and its binding partner PRC1 in organized central spindle midzone formation. *Embo J.* 23, 3237–48.
- 64 Peters, N. T. and Kropf, D. L. (2006). Kinesin-5 motors are required for organization of spindle microtubules in *Silvetia compressa* zygotes. *BMC Plant Biol.* 6, 19.
- 65 Cui, W., Sproul, L. R., Gustafson, S. M., Matthies, H. J., Gilbert, S. P. and Hawley, R. S. (2005). *Drosophila nod* protein binds preferentially to the plus ends of microtubules and promotes microtubule polymerization in vitro. *Mol. Biol. Cell* 16, 5400–5409.
- 66 Desai, A., Verma, S., Mitchison, T. J. and Walczak, C. E. (1999). Kin I kinesins are microtubule-destabilizing enzymes. *Cell* 96, 69–78.
- 67 Endow, S. A., Kang, S. J., Satterwhite, L. L., Rose, M. D., Skeen, V. P. and Salmon, E. D. (1994). Yeast Kar3 is a minus-end microtubule motor protein that destabilizes microtubules preferentially at the minus ends. *Embo J.* 13, 2708–2713.
- 68 Newton, C. N., Wagenbach, M., Ovechkina, Y., Wordeman, L. and Wilson, L. (2004). MCAK, a Kin I kinesin, increases the catastrophe frequency of steady-state HeLa cell microtubules in an ATP-dependent manner in vitro. *FEBS Lett.* 572, 80–84.
- 69 Walczak, C. E., Mitchison, T. J. and Desai, A. (1996). XKCM1: a *Xenopus* kinesin-related protein that regulates microtubule dynamics during mitotic spindle assembly. *Cell* 84, 37–47.
- 70 Karki, S., LaMonte, B. and Holzbaur, E. L. (1998). Characterization of the p22 subunit of dynactin reveals the localization of cytoplasmic dynein and dynactin to the midbody of dividing cells. *J. Cell Biol.* 142, 1023–34.
- 71 Maxwell, C. A., Keats, J. J., Crainie, M., Sun, X., Yen, T., Shibuya, E., Hendzel, M., Chan, G. and Pilarski, L. M. (2003). RHAMM is a centrosomal protein that interacts with dynein and maintains spindle pole stability. *Mol. Biol. Cell* 14, 2262–76.
- 72 Delcros, J. G., Prigent, C. and Giet, R. (2006). Dynactin targets Pavarotti-KLP to the central spindle during anaphase and facilitates cytokinesis in *Drosophila* S2 cells. *J. Cell Sci.* 119, 4431–41.
- 73 Aumais, J. P., Williams, S. N., Luo, W., Nishino, M., Caldwell, K. A., Caldwell, G. A., Lin, S. H. and Yu-Lee, L. Y. (2003). Role for NudC, a dynein-associated nuclear movement protein, in mitosis and cytokinesis. *J. Cell Sci.* 116, 1991–2003.
- 74 Cao, L. G. and Wang, Y. L. (1996). Signals from the spindle midzone are required for the stimulation of cytokinesis in cultured epithelial cells. *Mol. Biol. Cell* 7, 225–32.
- 75 de Gramont, A., Barbour, L., Ross, K. E. and Cohen-Fix, O. (2007). The spindle midzone microtubule-associated proteins Ase1p and Cin8p affect the number and orientation of astral microtubules in *Saccharomyces cerevisiae*. *Cell Cycle* 6, 1231–41.
- 76 Murata-Hori, M. and Wang, Y. L. (2002). Both midzone and astral microtubules are involved in the delivery of cytokinesis signals: insights from the mobility of aurora B. *J. Cell Biol.* 159, 45–53.
- 77 Norden, C., Mendoza, M., Dobbelaere, J., Kotwaliwale, C. V., Biggins, S. and Barral, Y. (2006). The NoCut pathway links completion of cytokinesis to spindle midzone function to prevent chromosome breakage. *Cell* 125, 85–98.
- 78 Straight, A. F., Cheung, A., Limouze, J., Chen, I., Westwood, N. J., Sellers, J. R. and Mitchison, T. J. (2003). Dissecting temporal and spatial control of cytokinesis with a myosin II inhibitor. *Science* 299, 1743–7.
- 79 Williams, B. C., Riedy, M. F., Williams, E. V., Gatti, M. and Goldberg, M. L. (1995). The *Drosophila* kinesin-like protein KLP3A is a midbody component required for central spindle assembly and initiation of cytokinesis. *J. Cell Biol.* 129, 709–23.
- 80 Fuller, B. G., Lampson, M. A., Foley, E. A., Rosasco-Nitcher, S., Le, K. V., Tobelmann, P., Brautigam, D. L., Stukenberg, P. T. and Kapoor, T. M. (2008). Midzone activation of aurora B in anaphase produces an intracellular phosphorylation gradient. *Nature* 453, 1132–6.
- 81 Janson, M. E. and Tran, P. T. (2008). Chromosome segregation: organizing overlap at the midzone. *Curr. Biol.* 18, R308–11.
- 82 O'Connell, C. B. and Wang, Y. L. (2000). Mammalian spindle orientation and position respond to changes in cell shape in a dynein-dependent fashion. *Mol. Biol. Cell* 11, 1765–74.